Research Square

Preprints are preliminary reports that have not undergone peer review.
They should not be considered conclusive, used to inform clinical practice,
or referenced by the media as validated information.

Teleconnection-driven predictability of the 2023 Brazilian heat wave

Omon A. Obarein
Kent State University https://orcid.org/0000-0002-6702-1143
Chibuike C. Ibebuchi
Department of Mathematics; Morgan State University, Baltimore, Maryland, USA
https://orcid.org/0000-0001-6010-2330
Alindomar L. Silva
ClimRISE Laboratory, Department of Geography; Kent State University, Kent, Ohio,
Amobichukwu C. Amanambu
acamanambu@ua.edu

Department of Geography and the Environment; University of Alabama, Tuscaloosa, USA
https://orcid.org/0000-0001-8798-189X

Research Article

Keywords: Heat waves, Teleconnections, Predictability, Brazil, LSTM, Air-mass typing, GWTC-2

Posted Date: March 25th, 2026

DOI: https://doi.org/10.21203/rs.3.rs-9204134/v1

License: This work is licensed under a Creative Commons Attribution 4.0 International License.
Read Full License

Additional Declarations: The authors declare no competing interests.

Abstract

Understanding the predictability and humidity characteristics of South American heat extremes remains a key challenge as their frequency accelerates under global warming. Here, we combine temperature regionalization, air-mass typing, and a teleconnection-driven LSTM framework to investigate these questions, using Brazil's record-breaking November 2023 heat wave as a focal case. Area-mean temperatures during the event exceeded the 1940–2023 climatology by ~ 2°C, and a new national record of 44.8°C was reported. Using rotated principal component analysis, we identify three temperature-coherent regions across Brazil and show that the November 2023 event was exceptional in affecting all regions simultaneously. Composite analyses reveal that positive temperature extremes are consistently preceded by an intensified, westward-displaced South Atlantic Subtropical High, which suppresses convection and enhances surface heating through subsidence. The event also coincided with the lowest nationwide November soil moisture since 1964, consistent with land-atmosphere feedbacks that amplify extreme heat. Using the Gridded Weather Typing Classification (GWTC-2), we distinguish dry heat over the central interior from humid heat along the northeastern Atlantic coast, a distinction with direct implications for health risk assessment. Finally, we demonstrate that selected oceanic indices explain approximately 78% of the variability in temperature extremes within a Long Short-Term Memory neural network, revealing substantial teleconnection-driven predictability. These results highlight that Brazilian heat extremes arise from coupled land-atmosphere-ocean processes and that this predictability can support improved early warning systems.

1. Introduction

Extreme temperature events such as heat waves have been aggravated by the background rise in average global temperatures (Perkins and Alexander 2013; Lee et al. 2020), driven mostly by increased atmospheric concentrations of greenhouse gases. In fact, globally, 2023 was the warmest year on record, with the global average near surface temperature reaching 1.45°C above the 1850–1900 baseline (WMO 2024), underscoring the pace of recent warming. The past decade (2014–2023) now represents the warmest ten-year period in the observational record (NASA 2024; WMO 2024). Concurrent with projected increases in global temperatures, climate models now project that the frequency, intensity, and duration of heat waves will increase at least up to the end of this century (Tebaldi et al. 2006; Perkins-Kirkpatrick and Lewis 2020; Stocker et al. 2021). These trends have been particularly pronounced in Brazil, where an urban-scale analysis reported increases in heat wave frequency from 0 to 3 events per year in the 1970s to 3 to 11 events per year in the 2010s across the 14 most populous urban areas (Monteiro dos Santos et al. 2024).

It was within this context of accelerating global warmth that Brazil experienced an exceptional heatwave in November 2023, which exemplified these intensifying trends. Average temperatures exceeded the 1940–2023 climatology by 2°C, and a new national record of 44.8°C was set at Araçuaí (Instituto Nacional de Meteorologia 2023; Pampuch et al. 2025). The event represented the largest positive temperature anomaly recorded in any spring or early summer month since 1940, with some locations

experiencing departures of up to 4°C above the long-term mean (Fig. 1). Warm conditions began emerging in September at the onset of spring and progressively expanded to near-total spatial coverage by November, signaling a sustained and spatially extensive thermal anomaly across the country (Marengo et al. 2025). The heatwave was linked to a persistent high-pressure system and atmospheric blocking, potentially connected to the 2023–2024 El Niño event, which suppressed cloud formation and enhanced descending air motion (Ivanovich et al. 2025; Marengo et al. 2025). Antecedent drought conditions further amplified temperatures by reducing soil moisture and partitioning more solar energy into sensible heat flux (Ivanovich et al. 2025; Pampuch et al. 2025). The extreme heat resulted in an estimated 1,392 excess deaths in Rio de Janeiro alone (Fernandez-Medina et al. 2025).

Heat waves, defined as sustained periods of hotter-than-normal temperatures (Meehl and Tebaldi 2004; Perkins and Alexander 2013), exert multifaceted impacts, transcending ecological and human dimensions. Ecosystems bear the brunt of prolonged high temperatures, with increased susceptibility to wildfires and disruptions in flora and fauna (Stillman 2019; Smale et al. 2019). Heat waves also carry economic repercussions by disrupting agriculture, straining water supplies, and threatening food storage and energy systems (Garcia-Leon et al. 2021; Xia et al. 2018).

In human health, heat waves are one of the leading causes of climate-induced mortality (Cvijanovic et al. 2023), especially among vulnerable populations such as the elderly and children (Gronlund et al. 2014; Li et al. 2015). Because humidity changes human physiological experience of heat, the co-occurrence of extreme humidity and heat waves tend to have a more debilitating effect than dry heat waves on human heat stress and thermoregulation (Matthews 2018; Wang et al. 2021). Humid (or wet or moist) heat waves are generally associated with heightened risks of cardiopulmonary diseases, and a surge in heat-related illnesses (Lowe et al. 2011; Gasparrini et al. 2012; Kenney et al. 2014; Sheridan and Lee 2018).

Across different climate regions, heat waves are typically associated with a large-scale, persistent high pressure, characterized by descending air, which compresses and warms adiabatically, inhibiting cloud formation, and leading to an increase in temperature at the surface (Tomczyk and Bednorz 2016). If the high-pressure system becomes stationary over a region for an extended period, it can initiate an atmospheric blocking event that traps heat and blocks cool air advection and other normal atmospheric circulation. Most continental extratropical heat waves, such as the 2003, 2015, and 2022 European summer heat waves, have all been linked to an atmospheric blocking event (Black et al. 2004; Souch and Grimmond 2004; Pezza et al. 2012; Ibebuchi and Abu 2023).

Unlike the mid-latitudes where pressure systems exhibit significant seasonal variability, tropical heat waves are generally associated with anomalous displacement in the intertropical convergence zone (ITCZ), whose seasonal north-south shifts control the location and intensity of the Equatorial Low (and localized high pressure systems) (Geirinhas et al. 2018; Costa et al. 2022). In monsoonal regions where pre-monsoon heat waves are common, drought conditions, at the end of a long dry season of significant soil moisture deficit, can cause high pressure to persist overland, creating conditions conducive to higher temperatures. This feature is common in the pre-monsoon heat waves of India (Rohini et al. 2019;

Satyanarayana and Rao 2020; Naveena et al. 2021) and West Africa (Ringard et al. 2013; Batté et al. 2018).

Marengo et al. (2025) study of the November 2023 Brazilian heat wave focused on the temporal evolution of atmospheric circulation and local to regional land surface factors that contributed to the heat wave between August to December. They found that high pressure system over central South America suppressed cloud formation, increased descending air motion, and led to extreme warming. Extreme temperatures were amplified by drought conditions by reducing soil moisture and driving more solar energy into sensible heat flux. Ivanovich et al. (2025) used reanalysis and high-resolution projections to diagnose the Rio de Janeiro–focused November 2023 heatwave, attributing it mainly to atmospheric blocking, soil-moisture declines, and elevated SSTs reducing coastal cooling.

Despite growing attention to Brazilian heat waves, three important gaps remain. First, prior studies of this event (Marengo et al. 2025; Ivanovich et al. 2025) focused on synoptic evolution and regional land-surface forcing but did not distinguish between dry and humid heat regimes, a distinction that fundamentally alters the severity, persistence, and mortality risk associated with extreme heat (Russo et al. 2017; Dahl et al. 2019). Second, while teleconnections between oceanic modes and South American climate have been noted qualitatively, their capacity to quantitatively predict Brazilian temperature extremes has not been tested in a predictive framework. Third, the November 2023 event was dynamically unusual in its pan-continental coherence, affecting all of Brazil's major climate zones simultaneously, yet the mechanisms enabling such spatial extent remain unexplored.

This study addresses these gaps through three specific objectives. (1) To diagnose the large-scale atmospheric circulation patterns and land-surface conditions, particularly soil moisture, associated with temperature extremes across Brazil's distinct climate zones, and to identify the mechanisms that enabled the pan-continental coherence of the November 2023 event. (2) To distinguish dry from humid heat regimes across Brazil during the heat wave using the Gridded Weather Typing Classification (GWTC-2). (3) To evaluate teleconnections between Brazilian temperature extremes and large-scale oceanic and climate mode indices, and to assess the predictability of these extremes using the identified teleconnections as inputs to a Long Short-Term Memory (LSTM) neural network. Together, these objectives aim to advance understanding of the coupled land-atmosphere-ocean processes governing Brazilian heat extremes and to explore pathways toward improved prediction and early warning.

2. Data and Methods

2.1. Data

This study uses 2-m mean monthly air temperature from ERA5 reanalysis (Hersbach et al. 2020) over Brazil (5° N–35° S, 74° W–34° W) for 1940–2023 at 0.25° × 0.25° resolution. Additional ERA5 fields, mean sea level pressure (MSLP), 1000- and 850-hPa geopotential height, and 850-hPa u and v winds, were taken for a larger domain (47° N–74° S, 162° W–34° E) to characterize large-scale circulation

during Brazilian heatwaves. Monthly indices of key climate modes were obtained from NOAA's Climate Prediction Center and analyses were restricted to 1950–2019, when most indices are available. All datasets were subset to September–December of each year to focus on the heatwave month and adjacent months.

2.2. Temperature Regionalization over Brazil

Monthly temperature was first converted to anomalies by subtracting the long-term mean at each grid point to remove the background trend and emphasize variability. A rotated S-mode principal component analysis (PCA) was then applied to these anomalies for the spring and early summer months to identify temperature-coherent regions. The correlation matrix of gridpoint temperatures was decomposed via singular value decomposition into eigenvectors (spatial patterns) and principal component (PC) scores (their temporal evolution). Loadings were iteratively rotated to align components with physically meaningful regional patterns, and a set of rotated components were retained when all their congruence coefficient with the original correlation vectors was ≥ 0.92 (Richman 1986; Ibebuchi and Richman 2023).

The regionalization was performed in a fuzzy manner, which, compared with traditional classification techniques, produces regions that do not have sharply defined boundaries. This technique captures in inherent overlap, continuity, and transition of climatic conditions and atmospheric circulation, so that each location belongs to multiple temperature regions with varying membership probabilities (Ibebuchi and Abu 2023; Ibebuchi and Richman 2023).

2.3. Atmospheric circulation patterns associated with temperature anomalies/regimes

Compositing, following an environment-to-circulation approach (Yarnal 1993; Lee et al. 2024), was used to identify circulation patterns associated with the November 2023 heatwave. For each temperature region, PC scores were used to define a positive (warm) and negative (cold) phase. Positive (negative) phases were defined as months with PC scores at or above the 95th percentile (at or below the 5th percentile), following common practice of using distribution tails of an EOF/PC-derived index to isolate the strongest realizations for composite analysis (Ding et al. 2023). For both phases in each region, composite maps were constructed from mean monthly anomalies (relative to 1940–2023) of 2-m temperature, MSLP, 850-hPa winds, and 1000–850-hPa thickness. Restricting composites to the upper and lower 5% of PC scores isolates months when the regional temperature patterns are most strongly expressed, thereby highlighting the clearest associated atmospheric signals.

2.4. Land Surface and Humidity Characteristics

Wet-bulb temperature (WBT) is a widely used heat-stress index that incorporates humidity and temperature, providing a more realistic measure of human thermal strain than temperature alone (e.g., Coffel et al. 2019; El Khayat et al. 2022). Here, Dry Warm (DW) and Humid Warm (HW) air masses from version 2 of the Gridded Weather Typing Classification (GWTC-2) are used to distinguish dry and humid heat. GWTC-2 is a multivariate classification that assigns each grid point and day to one of 11 weather

types. (see Lee 2014, 2020). DW days fall in the bottom 25th percentile of dew point and top 75th percentile of surface temperature for that location and time of year, while HW days fall in the top 75th percentile of both temperature and dew point, approximating high-WBT conditions. The GWTC-2 incorporates sea level pressure, cloud cover and wind, important atmospheric variables driving heat waves.

To examine land–atmosphere coupling, monthly soil moisture trends and the November 2023 soil moisture anomaly were calculated over Brazil. Volumetric soil moisture ($m^3\ m^{-3}$) in the upper soil layer (0–7 cm; Layer 1) from ERA5 reanalysis (ECMWF) for 1940–2023 (September–December) was used to assess whether anomalously dry soils contributed to the November 2023 heatwave.

2.5. Brazilian temperature variability and climate modes/oscillations: Association and predictability

Anomalous temperatures are often modulated by large-scale climate modes operating on seasonal to decadal timescales. To assess these links, monthly time series of selected climate modes were correlated with regional PC scores using Pearson's correlation, and only modes with $|r| \geq 0.6$ were retained as predictors. The predictability of PC scores was then evaluated with a Long Short-Term Memory (LSTM) model (Hochreiter and Schmidhuber 1997), using these climate-mode indices as inputs. Data were split into an 80% training set (1950–1998) and 20% testing set (1999–2019), with 10% of the training period used for validation and tuning key hyperparameters (e.g., neuron count, learning rate, batch size) using objective Keras tuner.

3. Results

3.1. Brazilian Spring and Early Summer Temperature Regions (1940–2023)

The regionalization of Brazilian spring and early summer (September to December) surface temperature produced three coherent regions using ERA5 data (Fig. 2). Region 1 lies at the heart of the vast Tropical Savanna Climate in central Brazil, characterized by year-round warm temperatures and a well-defined precipitation seasonality. Region 2 has large loading magnitudes over southern Brazil where Humid sub-tropical climate conditions prevail. The temperature in this region is not only the coldest but also the most variable, exhibiting a significant annual temperature range, with little precipitation seasonality. Being proximate to the equator, Region 3 spans humid tropical and semi-arid climate regimes in northern Brazil. The Amazon portion is hot and wet year-round with little annual temperature range, with typical stations exceeding 28°C in all months. In contrast, the northeastern branch has a pronounced wet season from March–July (Stosic et al. 2025), while the interior Northeast is characterized by a semi-arid climate.

The fuzzy classification is evident in the within-region heterogeneity: PC loadings decrease from high values in regional cores to lower values at the periphery, and many grid points can belong to multiple regions. For example, the state of São Paulo in southeastern Brazil contains locations that belong to all three temperature regions.

The monthly PC score time series for each region (Fig. 3) represents the evolving magnitude of its temperature pattern, with positive scores indicating positive anomalies and negative scores indicating negative anomalies. In Region 1, positive anomalies are most common in September–October, while November–December are typically dominated by negative anomalies; this makes the November 2023 event highly unusual, the second-largest positive November–December anomaly since 1940. Region 2 shows the opposite seasonal behavior, with November–December dominated by positive anomalies, especially over the last three decades, and the exceptionally large November 2023 anomaly continuing this recent trend. In Region 3, the November 2023 anomaly is likewise strongly positive and consistent with the recent tendency toward more frequent warm anomalies.

All three regions display distinct temperature regimes, reflected in differences in the sign and magnitude of their monthly PC scores. Yet November 2023 stands out with consistently high scores in every region. When PC scores are averaged across regions (Fig. 4), a coherent warming signal emerges, especially the pervasive positive scores over the last three decades. Within this context, November 2023 shows significantly higher anomalies, particularly in Regions 1 and 2, where November 2023 PC scores are the highest on record since 1940, demonstrating both the intensity and broad spatial extent of the heatwave.

3.2. Humidity and Soil Moisture Characteristics

Figure 5a maps the spatial anomaly of Humid Warm (W), Dry Warm (DW), and Warm (W) days during the heat wave, relative to the long-term mean for November (1940–2023). During the heat wave, warm air masses (AMs) increased by up to 18 days in the month. HW days were dominant in the Tropical Rainforest climate region in Northern and Northwestern Brazil, especially along the coast (Region 3), while excess DW days were focused over the hot, drier Tropical Savanna in central Brazil (Region 1).

The nationwide averaged time-series of anomalous November AMs is shown in Fig. 5b. HW days overwhelmingly dominated the 2023 event: anomalous HW frequency in November 2023 was the largest of any November since 1940 and roughly 2–3 times higher than DW and W days, which themselves reached their highest levels in two decades. Brazil's equatorial climate is hot year-round, with abundant moisture from the Atlantic, creating the ideal hotspot for HW AMs, and the development of humid heat waves. Similarly, and unsurprisingly, DW hotspots develop in the hot but drier Tropical Savanna climate (Ha et al. 2022; Fan et al. 2024). DW AMs are characteristic of dry heat waves that tend to have longer durations than humid heat waves (Russo et al. 2017; Li et al. 2023). In contrast, humid heat waves tend to be shorter but more intense due to humidity's amplifying effect on heat stress (Russo et al. 2015; Buzan and Huber 2020). In our results (Fig. 1), this contrast appears as a rapid post-September decline in equatorial temperature anomalies versus the season-long persistence of warm anomalies over the savanna.

Figure 6 shows November 2023 volumetric soil moisture anomalies across Brazil. During the heatwave, soil moisture reached its lowest November values since 1964 nationwide, with the largest deficits over the continental interior and equatorial belt and weaker deficits near the coasts. These anomalies occurred against a broader trend of declining soil moisture (Fig. 6b), consistent with regional warming over the past two decades, and likely intensified the heatwave, an amplification mechanism also found for the 2003 European event and the 2009–2010 China heatwave (Fischer et al. 2007; Jiang et al. 2022).

3.3. Atmospheric circulation patterns associated with Brazilian heat wave

Composite temperature anomaly maps for each region are shown in Fig. 7. The dates used for the positive and negative phases are listed in Supplementary Tables S1–S3. As expected, positive PC phases correspond to positive temperature anomalies over Brazil, and negative phases to negative anomalies, in all three regions. In Region 1 (both phases) and in the negative phase of Region 3, the composites exhibit a weak zonal dipole, with opposing temperature anomalies across the domain.

Figure 8 shows composite anomalies of MSLP, 850-hPa winds, and atmospheric layer thickness for the positive and negative PC phases in each region. In all regions, positive phases feature enhanced layer thickness collocated with warm temperature anomalies at regional cores, while negative phases show reduced thickness over cool temperature anomalies. The weak dipole seen in Fig. 7 reappears in layer thickness, highlighting a regional seesaw in which central Brazil warms while the south cools, or equatorial Brazil cools while the humid subtropical south warms. This pattern is consistent with large-scale variability linked to SST anomalies, SACZ shifts, and ENSO (Wong et al. 2023; Kim et al. 2025).

In Region 1, the positive phase is associated with a South Atlantic high and divergent easterly–northeasterly winds, whereas the negative phase shows a South Atlantic low off southeast Brazil with convergent flow, shallow thickness, and cooler conditions. The positive phase of region 2 features a broad South Atlantic low with converging winds and a South Pacific high with divergence; its negative phase shows a strong high centered over anomalously cool, shallow air and a low in the central Pacific. High pressure co-located with cool anomalies suggests surface radiative cooling under clear, stable conditions. In Region 3, the positive phase displays a high over the southeastern Pacific and a low over the South Atlantic, while the negative phase features a South Atlantic high, with negative temperature anomalies over northern Brazil teleconnected to very warm anomalies in the humid subtropical south.

3.4. Association between Brazilian temperature anomalies (PC Scores) and selected climatic modes

The correlation coefficient between PC scores, representing the magnitude of the dominant temperature patterns in Brazil, and twenty climate indices is presented in Table 1. Of the three regions, Region 3 had the strongest correlation with the selected climate indices, while Region 1 was the least correlated with climate indices. The Western Hemisphere Warm Pool (WHWP), the Tropical Northern Atlantic index, and the Tropical Southern Atlantic index (TNA and TSA), the Atlantic Multidecadal Oscillation (AMO), the

North Tropical Atlantic index (NTA), and the Caribbean Index (CAR) all have positive and statistically significant correlation with temperature patterns across all regions. Of these modes, the WHWP (0.82) and the CAR (0.71) have the strongest positive correlation with the climate indices, especially in Region 3. The spatial extent of these climate indices is shown in the Appendix (Figure S1)

All other indices are negatively correlated with temperature patterns across all Brazilian temperature regions. In general, the correlations for all the regions agree in terms of sign of correlation but with differing magnitudes, except with the Pacific Decadal Oscillation (PDO) where correlation with temperature patterns in Region 1 is negative but positive and statistically significant in Region 3. The East Central Tropical Pacific SST (Niño 3.4) had a strong positive correlation with temperature patterns in Regions 2 and 3, but it is only weakly correlated with temperature in Region 1.

Table 1—*Pearson's correlation coefficient between Regional PC Scores in each temperature coherent region and climate indices (1950 – 2019). Shades of Blue (Red) indicate positive (negative) correlation. Bold font marks statistical significance.*

Monthly Indices of Climate Modes	Region		
	1	2	3
Atlantic Meridional Mode (AMM)	0.19	0.15	**0.36**
Atlantic Multidecadal Oscillation (AMO)	**0.45**	**0.33**	**0.61**
Arctic Oscillation (AO)	-0.01	0.10	-0.09
Caribbean Index (CAR)	**0.41**	**0.48**	**0.71**
Eastern Atlantic/Western Russia (EA/WR)	-0.06	0.00	-0.19
East Pacific/North Pacific Oscillation (EP/NP)	-0.16	-0.13	-0.06
North Atlantic Oscillation (NAO)	0.02	0.04	0.00
East Central Tropical Pacific SST (Niño 3.4)	0.11	**0.35**	**0.53**
North Pacific Pattern (NP)	0.00	-0.01	-0.06
North Tropical Atlantic Index (NTA)	**0.26**	**0.44**	**0.61**
Pacific Warm pool Region	0.16	**0.58**	**0.44**
Pacific Decadal Oscillation (PDO)	-0.14	**0.13**	**0.3**
Pacific North American Index (PNA)	0.06	0.03	**0.27**
Tropical Northern Atlantic Index (TNA)	**0.31**	**0.39**	**0.63**
Tropical Southern Atlantic Index (TSA)	**0.30**	**0.56**	**0.25**
Western Hemisphere Warm Pool (WHWP)	**0.42**	0.54	**0.82**
Western Pacific Index (WP)	-0.17	-0.14	0.08

3.5. Predictability of Brazilian temperature anomalies from climate/oceanic indices using neural networks

After examining the association between climate indices and temperature variability in Brazil, we evaluate the predictability of temperature patterns in Region 3 by the climate indices using the predictive long short-term memory (LSTM) deep learning model. All climate indices with a correlation coefficient greater than 0.60 were included in the predictive model. These include, WHWP, CAR, AMO, TNA, NTA, and

Niño 3.4. The trained model was tested on the last 30% of the data (1999–2019), and Fig. 9 shows the time series of the actual PC scores and the predicted PC scores for Region 3. The model produced an R^2 of 0.776, indicating that the selected climate indices explain about 78% of the variability in PC scores. In addition, there is a strong positive correlation of 0.89 (not shown) between the actual and predicted PC scores in the testing period.

4. Discussion

Brazil's extensive latitudinal range creates heterogeneous climate and temperature regimes, necessitating regionalization to understand spatial temperature variability. This analysis also aimed to determine whether atmospheric heat-wave drivers were common across Brazil's main climate zones. We found that temperature anomalies evolved differently across the three regions, indicating that each may be subject to distinct temperature drivers, or to similar drivers acting with varying intensities. This is supported by the clear dipole structure in the anomaly field, with contrasting temperature anomalies between the southern vs. northern Brazil and southern vs. central regions (Fig. 7). Yet the November 2023 heat wave affected all Brazilian regions simultaneously. This scope is exceptional given that historical Brazilian heat waves have typically been more regional than continental. At the same time, it aligns with an emerging pattern of large, multi-region events spanning the whole country.

Brazilian heat waves have been linked to a northward displacement of the Intertropical Convergence Zone (ITCZ), which suppresses the South American Monsoon System (SAMS), weakens moisture convergence, reduces cloud cover, and allows intense insolation. A weakened SAMS is also associated with a strengthened South Atlantic Subtropical High (SASH), a semi-permanent high-pressure cell over the South Atlantic, that promotes surface heating through subsidence, diminished rainfall, and clear skies (Geirinhas et al. 2018, 2019). Consistent with this framework, our results show an anomalously strong South Atlantic high co-occurring with strong positive temperature anomalies over central and northern Brazil. Prior work further indicates that a westward-oriented SASH reduces frontal passages over south and southeastern Brazil, enabling hot extremes to build under low-humidity conditions (Geirinhas et al. 2018). Our composites likewise show a markedly westward-displaced SASH, supporting the literature and linking elevated temperatures across central and southern Brazil to this western, intensified high-pressure system.

Drought can intensify large-scale circulation shifts through regional land–atmosphere coupling (Schumacher et al. 2019; Mukherjee and Mishra 2021; Jiang et al. 2022; Geirinhas et al. 2022). In the Amazon, Costa et al. (2022) found that all ten heat waves between 1979–2018 coincided with extreme drying. Likewise, this study found that the November 2023 heat wave occurred alongside the lowest nationwide soil moisture levels since November 1964. Under drought, negative soil-moisture anomalies reduce evapotranspiration, suppress cloud formation, and increase the amount of solar radiation reaching the surface. With less energy partitioned into latent heat (evaporation) and more into sensible heating, near-surface temperatures rise. This feedback can contribute roughly 30–70% of the atmospheric temperature anomaly and heat-wave intensity (Zhang and Wu 2011) and has been

documented in the anomalous outgoing solar radiation during the 2003 European heat wave (Black et al. 2004) and in the 2021 western U.S. heat wave. In the Amazon, a key contributor to compound drought–heat extremes is deforestation (Marengo et al. 2011, 2018). Since, rainforests recycle up to ~ 56% of precipitation via evapotranspiration (Aragão 2012), forest loss disrupts this moisture-recycling system and reinforces the same positive feedback loop.

Because the atmosphere and ocean form a coupled system, air–sea interactions can trigger or reinforce regional circulation patterns through large-scale climate modes. The modes that correlate strongly with, and can skillfully predict, anomalous Brazilian temperatures, particularly over the Amazon, are often tied to positive Atlantic SSTAs. For example, SST gradients between the Tropical South Atlantic (TSA) and Tropical North Atlantic (TNA) can shift the ITCZ and modulate the strength of the SAMS, suppressing convection while enhancing surface warming (Garcia and Kayano 2010). The Western Hemisphere Warm Pool (WHWP), which is influenced by ENSO, can alter low-level moisture flux into Central America and affect Amazon rainfall variability (Wang and Enfield 2003; Wang et al. 2007). Cataldi et al. (2025) further suggest that WHWP anomalies may indirectly influence Brazilian temperature extremes by modulating blocking events or patterns of moisture convergence linked to the ITCZ. Finally, the strong correlation of the AMO with temperature extremes over Northeastern Brazil (Region 3) aligns with studies linking positive AMO phases to reduced precipitation and elevated temperatures in that region (Kayano and Andreoli 2004; Knight et al. 2006).

The strong correlations between these Atlantic-dominated climate modes and Brazilian temperature extremes translate into substantial predictive skill. The LSTM model, using WHWP, CAR, AMO, TNA, NTA, and Nino 3.4 as inputs, explains approximately 78% of the variability in Region 3 PC scores during the independent testing period (1999–2019). This result is notable because the predictors are exclusively oceanic indices, yet they capture the majority of interannual variability in temperature extremes over northern and northeastern Brazil. The physical basis for this skill lies in the dynamical chain identified above: anomalous Atlantic SSTs modulate the ITCZ position and SASH intensity (Garcia and Kayano 2010), which in turn control subsidence, cloud cover, and surface heating over Brazil. That oceanic boundary conditions alone account for this level of variability suggests that Brazilian heat extremes are more tightly coupled to remote ocean forcing than previously quantified. While Cataldi et al. (2025) identified qualitative links between teleconnection patterns and Brazilian climate extremes, our results provide the first quantitative demonstration that these indices carry sufficient information to predict temperature extremes with high skill. This finding is consistent with the demonstrated utility of oceanic predictors for subseasonal-to-seasonal heat wave forecasting in other tropical regions (Batte et al. 2018) and suggests that prediction systems ingesting real-time SST information could provide actionable lead times for heat wave early warning in Brazil.

Not all heat waves are created equally; distinguishing between moist and dry heat is essential for understanding event severity, persistence, and associated mortality (Russo et al. 2017; Dahl et al. 2019). Prior studies show that dry heat waves are more common in arid regions due to entrainment of hot, dry air, whereas humid heat waves often reflect advection of hot, moisture-laden air from nearby water

bodies (Xu et al. 2021; Rastogi et al. 2020). This corroborates with our findings of excess DW AMs in the drier Cerrado belt (Region 1), where divergent winds indicate high pressure and subsidence that warm adiabatically. In contrast, the composites in Fig. 8 show clear landward advection of moist air from Brazil's equatorial coast into the northeastern region, where some locations experienced up to 18 excess HW days.

The novel use of GWTC-2 AMs offers advantages over traditional heat-stress indices (e.g., wet-bulb temperature) for attribution and explanation. Because heat waves are often evaluated in terms of duration and repeated exposure, counting excess DW and HW days is direct and interpretable. More importantly, GWTC-2 is multivariate, incorporating several near-surface atmospheric variables, thereby providing a synoptic context rather than a single thermal-stress metric. In addition, its air-mass definitions are relative to local seasonal climatology, improving comparability across different climates.

As global warming increases atmospheric moisture-holding capacity, HW days have risen across most regions (Lee 2020) and are projected to increase further. Under high-emissions scenarios, parts of the Earth may, by late century, periodically exceed thresholds for human thermoregulation (Matthews 2018; Schär 2016).

5. Summary and Conclusion

This study investigated the teleconnection-driven predictability, humidity characteristics, and atmospheric forcing of Brazilian heat extremes, using the record-breaking November 2023 event as a focal case. The atmospheric circulation analysis reveals that extreme heat across Brazil is consistently associated with an intensified, westward-displaced South Atlantic Subtropical High, compounded by severe soil moisture deficits that reached their lowest nationwide November levels since 1964. The November 2023 event was exceptional in its pan-continental coherence, simultaneously affecting all three identified temperature regions, a pattern that contrasts with the more regionally confined heat waves in the historical record. The GWTC-2 air-mass classification further reveals distinct dry and humid heat regimes during the event, with dry heat concentrated over the central Cerrado and humid heat along the northeastern Atlantic coast. This spatial differentiation is relevant for risk assessment, as dry and humid heat waves differ in duration, intensity, and health impacts (Russo et al. 2017; Dahl et al. 2019).

Most significantly for prediction, selected oceanic teleconnection indices explain approximately 78% of the variability in temperature extremes over northern and northeastern Brazil within an LSTM neural network framework. The dominant predictors, WHWP, CAR, AMO, TNA, NTA, and Nino 3.4, are predominantly Atlantic SST-related modes that influence Brazilian heat through modulation of the ITCZ and SASH. This level of ocean-driven predictive skill has not been previously quantified for Brazilian heat extremes and points toward a viable pathway for subseasonal-to-seasonal heat wave forecasting in the region. Future work should incorporate lagged predictor-response relationships to assess operational lead times, integrate land-surface variables such as soil moisture into the predictive framework to

capture compound drought-heat interactions, and extend the analysis beyond Region 3 to evaluate whether similar teleconnection-based skill holds across southern and central Brazil.

Declarations

Author contributions

O.A. Obarein conceptualized the study, performed the data analysis, developed the LSTM predictive framework, and wrote the original draft. C.C. Ibebuchi contributed to the GWTC-2 weather type classification methodology and reviewed the manuscript. A.L. Silva contributed to data processing and visualization. A.C. Amanambu supervised the research, contributed to the conceptual framing, and critically revised the manuscript. All authors read and approved the final manuscript.

Acknowledgement

The authors thank Dr Cameron Lee for his contribution to data availability and his supervision during the early conceptualization of this study.

Competing interests The authors declare no competing interests.

Data availability

The ERA5 reanalysis data used in this study are available from the Copernicus Climate Data Store (https://cds.climate.copernicus.eu). Sea surface temperature-based teleconnection indices were obtained from NOAA Physical Sciences Laboratory (https://psl.noaa.gov). The GWTC-2 global weather type classification data are available from the Kent State University web platform (https://www.personal.kent.edu/~cclee/gwtc2global.html).

References

1. Aragão LE (2012) The rainforest's water pump. Nature 489:217–218. https://doi.org/10.1038/nature11485
2. Batté L, Ardilouze C, Déqué M (2018) Forecasting West African heat waves at subseasonal and seasonal time scales. Mon Weather Rev 146(3):889–907
3. Black E, Blackburn M, Harrison G, Hoskins B, Methven J (2004) Factors contributing to the summer 2003 European heatwave. Weather 59(8):217–223
4. Buzan JR, Huber M (2020) Moist heat stress on a hotter Earth. Annu Rev Earth Planet Sci 48(1):623–655
5. Cataldi M, Sancho L, Esposte Coutinho P, da Fonseca Aguiar L, Galves VLV, Guida A (2025) Teleconnection Patterns and Synoptic Drivers of Climate Extremes in Brazil (1981–2023).

Atmosphere 16(6):699

6. Coffel ED, Horton RM, Winter JM, Mankin JS (2019) Nonlinear increases in extreme temperatures paradoxically dampen increases in extreme humid-heat. Environ Res Lett 14(8):084003
7. Costa DF, Gomes HB, Silva MCL, Zhou L (2022) The most extreme heat waves in Amazonia happened under extreme dryness. Clim Dyn 59(1):281–295
8. Cvijanovic I, Mistry MN, Begg JD, Gasparrini A, Rodó X (2023) Importance of humidity for characterization and communication of dangerous heatwave conditions. NPJ Clim atmospheric Sci 6(1):33
9. Dahl K, Licker R, Abatzoglou JT, Declet-Barreto J (2019) Increased frequency of and population exposure to extreme heat index days in the United States during the 21st century. Environ Res Commun 1(7):075002
10. Ding X, Chen G, Zhang P, Domeisen DI, Orbe C (2023) Extreme stratospheric wave activity as harbingers of cold events over North America. Commun Earth Environ 4(1):187
11. El Khayat M, Halwani DA, Hneiny L, Alameddine I, Haidar MA, Habib RR (2022) Impacts of climate change and heat stress on farmworkers' health: A scoping review. Front Public Health 10:782811
12. Fan X, Miao C, Wu Y, Mishra V, Chai Y (2024) Comparative assessment of dry-and humid-heat extremes in a warming climate: frequency, intensity, and seasonal timing. Weather Clim Extrem 45:100698
13. Fernandez-Medina RDF, Peixoto EM, Rodrigues D, Said R, Holanda CA, Freire CDS, Barreto ML et al (2025) Excess mortality associated with extreme heat in Rio de Janeiro, Brazil, 2023. Rev Panam Salud Publica 49:e76. https://doi.org/10.26633/RPSP.2025.76
14. Fischer EM, Seneviratne SI, Vidale PL, Lüthi D, Schär C (2007) Soil moisture–atmosphere interactions during the 2003 European summer heat wave. J Clim 20(20):5081–5099
15. Garcia SR, Kayano MT (2010) Some evidence on the relationship between the South American monsoon and the Atlantic ITCZ. Theor Appl Climatol 99(1):29–38
16. García-León D, Casanueva A, Standardi G, Burgstall A, Flouris AD, Nybo L (2021) Current and projected regional economic impacts of heatwaves in Europe. Nat Commun 12(1):5807
17. Gasparrini A, Armstrong B, Kovats S, Wilkinson P (2012) The effect of high temperatures on cause-specific mortality in England and Wales. Occup Environ Med 69(1):56–61
18. Geirinhas JL, Trigo RM, Libonati R, Coelho CA, Palmeira AC (2018) Climatic and synoptic characterization of heat waves in Brazil. Int J Climatol 38(4):1760–1776
19. Geirinhas JL, Trigo RM, Libonati R, Castro LC, Sousa PM, Coelho CA et al (2019) Characterizing the atmospheric conditions during the 2010 heatwave in Rio de Janeiro marked by excessive mortality rates. Sci Total Environ 650:796–808
20. Geirinhas JL, Russo AC, Libonati R, Miralles DG, Sousa PM, Wouters H, Trigo RM (2022) The influence of soil dry-out on the record-breaking hot 2013/2014 summer in Southeast Brazil. Sci Rep 12(1):5836

21. Gronlund CJ, Zanobetti A, Schwartz JD, Wellenius GA, O'Neill MS (2014) Heat, heat waves, and hospital admissions among the elderly in the United States, 1992–2006. Environ Health Perspect 122(11):1187–1192
22. Ha KJ, Seo YW, Yeo JH, Timmermann A, Chung ES, Franzke CL et al (2022) Dynamics and characteristics of dry and moist heatwaves over East Asia. npj Clim Atmos Sci 5(1):49
23. Hersbach H, Bell B, Berrisford P, Hirahara S, Horányi A, Muñoz-Sabater J et al (2020) The ERA5 global reanalysis. Q J R Meteorol Soc 146(730):1999–2049
24. Hochreiter S, Schmidhuber J (1997) Long short-term memory. Neural Comput 9(8):1735–1780
25. Ibebuchi CC, Abu IO (2023) Characterization of temperature regimes in Western Europe, as regards the summer 2022 Western European heat wave. Clim Dyn 61(7):3707–3720
26. Ibebuchi CC, Obarein OA, Abu IO (2024) Application of autoencoders artificial neural network and principal component analysis for pattern extraction and spatial regionalization of global temperature data. Mach Learn Sci Technol 5(1):015009
27. Instituto Nacional de Meteorologia (2023) *INMET Portal*. https://portal.inmet.gov.br/
28. IPCC (2021) *Climate Change 2021: The Physical Science Basis* (AR6 WGI), Summary for Policymakers / Chap. 11 (Weather and Climate Extreme Events). Cambridge University Press
29. Ivanovich CC, Sobel AH, Horton RM, Nunes AMB, da Rocha RP, Camargo SJ (2025) Physical drivers of the November 2023 heatwave in Rio de Janeiro. Weather Clim Dyn 6:1857–1874. https://doi.org/10.5194/wcd-6-1857-2025
30. Jiang L, Chen YD, Li J, Liu C (2022) Amplification of soil moisture deficit and high temperature in a drought-heatwave co-occurrence in southwestern China. Nat Hazards. https://doi.org/10.1007/s11069-021-05071-3
31. Kayano MT, Andreoli RV (2004) Decadal variability of northern northeast Brazil rainfall and its relation to tropical sea surface temperature and global sea level pressure anomalies. J Geophys Res Oceans 109:C11
32. Kenney WL, Craighead DH, Alexander LM (2014) Heat waves, aging, and human cardiovascular health. Med Sci Sports Exerc 46(10):1891
33. Kim HJ, Kim JS, Ham YG, Park JH, Milodowski D, Aragão LE, Williams M (2025) Anomalous temperature in North Tropical Atlantic linked to Brazilian Cerrado fires. npj Clim Atmos Sci 8(1):63
34. Knight JR, Folland CK, Scaife AA (2006) Climate impacts of the Atlantic multidecadal oscillation. Geophys Res Lett, *33*(17)
35. Jiménez-Muñoz JC, Mattar C, Barichivich J, Santamaría-Artigas A, Takahashi K, Malhi Y et al (2016) Record-breaking warming and extreme drought in the Amazon rainforest during the course of El Niño 2015–2016. Sci Rep 6(1):33130
36. Lee CC (2014) The development of a gridded weather typing classification scheme. Kent State University

37. Lee CC (2020a) The gridded weather typing classification version 2: A global-scale expansion. Int J Climatol 40(2):1178–1196
38. Lee CC (2020b) Trends and variability in airmass frequencies: indicators of a changing climate. J Clim 33(19):8603–8617
39. Lee CC, Obarein O, Sheridan SC, Smith ET, Adams R (2021) Examining trends in multiple parameters of seasonally-relative extreme temperature and dew point events across North America. Int J Climatol 41:E2360–E2378
40. Lee CC, Sheridan SC, Pirhalla DE, Ransibrahmanakul V, Dusek G (2024a) A novel applied climate classification method for assessing atmospheric influence on anomalous coastal water levels. Int J Climatol 44(7):2484–2504
41. Lee CC, Silva A, Ibebuchi C, Sheridan SC (2024b) The influence of air masses on human mortality in the contiguous United States. Int J Biometeorol. https://doi.org/10.1007/s00484-024-02745-y
42. Li M, Gu S, Bi P, Yang J, Liu Q (2015) Heat waves and morbidity: current knowledge and further direction-a comprehensive literature review. Int J Environ Res Public Health 12(5):5256–5283
43. Li L, Wang L, Feng T, Tang J, Huang J, Cai Z (2023) Multi-Index Analysis of Spatiotemporal Variations of Dry Heat Waves and Humid Heat Waves in China. Atmosphere 14(11):1660
44. Lowe D, Ebi KL, Forsberg B (2011) Heatwave early warning systems and adaptation advice to reduce human health consequences of heatwaves. Int J Environ Res Public Health 8(12):4623–4648
45. Marengo JA, Tomasella J, Alves LM, Soares WR, Rodriguez DA (2011) The drought of 2010 in the context of historical droughts in the Amazon region. Geophys Res Lett, *38*(12)
46. Marengo JA, Souza CM Jr, Thonicke K, Burton C, Halladay K, Betts RA et al (2018) Changes in climate and land use over the Amazon region: current and future variability and trends. Front Earth Sci 6:228
47. Marengo JA, Costa MC, Cunha AP, Espinoza JC, Jimenez JC, Libonati R, Miranda V, Trigo IF, Sierra JP, Geirinhas JL, Ramos AM, Skansi M, Molina-Carpio J, Salinas R (2025) Climatological patterns of heatwaves during winter and spring 2023 and trends for the period 1979–2023 in central South America. Front Clim 7:1529082. https://doi.org/10.3389/fclim.2025.1529082
48. Matthews T (2018) Humid heat and climate change. Prog Phys Geogr 42(3):391–405
49. Meehl GA, Tebaldi C (2004) More intense, more frequent, and longer lasting heat waves in the 21st century. Science 305(5686):994–997
50. Monteiro dos Santos D, Libonati R, Garcia BN, Geirinhas JL, Salvi BB, Lima e Silva E, Rodrigues JA, Peres LF, Russo A, Gracie R (2024) Twenty–first–century demographic and social inequalities of heat related deaths in Brazilian urban areas. PLoS ONE 19:e0295766. https://doi.org/10.1371/journal.pone.0295766
51. Mukherjee S, Mishra AK (2021) Increase in compound drought and heatwaves in a warming world. Geophys Res Lett, *48*(1), e2020GL090617.
52. NASA (2024) NASA analysis confirms 2023 as warmest year on record. https://www.nasa.gov/

53. Naveena N, Satyanarayana GC, Rao DB, Srinivas D (2021) An accentuated hot blob over Vidarbha, India, during the pre-monsoon season. Nat Hazards 105:1359–1373
54. Pampuch LA, Bueno PG, Reboita MS, Tomaziello ACN, Nunes AMP, Cardoso AA, Coelho CAS, Carpenedo CB, Vasconcelos FC Jr, Gomes HB, Pinheiro HR, Braga HA, Borges IVG, Custodio MS, da Silva ML, Llopart M, da Rocha RP, Ambrizzi T et al (2025) Mendes da Silva GA Brazil climate highlights 2023. Ann NY Acad Sci 1549:120–138. https://doi.org/10.1111/nyas.15394
55. Perkins SE, Alexander LV (2013) On the measurement of heat waves. J Clim 26(13):4500–4517
56. Perkins-Kirkpatrick SE, Lewis SC (2020) Increasing trends in regional heatwaves. Nat Commun 11(1):3357
57. Pezza AB, Van Rensch P, Cai W (2012) Severe heat waves in Southern Australia: synoptic climatology and large scale connections. Clim Dyn 38:209–224
58. Rastogi D, Lehner F, Ashfaq M (2020) Revisiting recent US heat waves in a warmer and more humid climate. Geophys Res Lett, *47*(9), e2019GL086736.
59. Ringard J, Rome S, Diedhiou A (2013) Retrospective and prospective study of the heat waves in West Africa. Threshold 24:26
60. Rohini P, Rajeevan M, Mukhopadhay P (2019) Future projections of heat waves over India from CMIP5 models. Clim Dyn 53:975–988
61. Russo S, Sillmann J, Fischer EM (2015) Top ten European heatwaves since 1950 and their occurrence in the coming decades. Environ Res Lett 10(12):124003
62. Russo S, Sillmann J, Sterl A (2017) Humid heat waves at different warming levels. Sci Rep 7(1):7477
63. Schär C (2016) The worst heat waves to come. Nat Clim Chang 6(2):128–129
64. Schumacher DL, Keune J, Van Heerwaarden CC, Vilà-Guerau de Arellano J, Teuling AJ, Miralles DG (2019) Amplification of mega-heatwaves through heat torrents fuelled by upwind drought. Nat Geosci 12(9):712–717
65. Satyanarayana GC, Rao DB (2020) Phenology of heat waves over India. Atmos Res 245:105078
66. Sheridan SC, Lee CC (2018) Temporal trends in absolute and relative extreme temperature events across North America. J Geophys Res Atmos 123(21):11–889
67. Smale DA, Wernberg T, Oliver EC, Thomsen M, Harvey BP, Straub SC et al (2019) Marine heatwaves threaten global biodiversity and the provision of ecosystem services. Nat Clim Chang 9(4):306–312
68. Souch C, Grimmond CSB (2004) Applied Climatology:'heat waves'. Prog Phys Geogr 28(4):599–606
69. Stillman JH (2019) Heat waves, the new normal: summertime temperature extremes will impact animals, ecosystems, and human communities. Physiology 34(2):86–100
70. Stosic B, Djurdjević V, Tošić I, da Silva ASA, Stosic T (2025) Quantifying the Rainy Season in the Brazilian Northeast Through a Modification of the Relative Entropy Method. Water 17(7):1086
71. Tebaldi C, Hayhoe K, Arblaster JM, Meehl GA (2006) Going to the extremes: an intercomparison of model-simulated historical and future changes in extreme events. Clim Chang 79(3):185–211

72. Tomczyk AM, Bednorz E (2016) Heat waves in Central Europe and their circulation conditions. Int J Climatol, *36*(2)
73. Valverde MC, Rosa MB (2023) Heat waves in São Paulo State, Brazil: Intensity, duration, spatial scope, and atmospheric characteristics. Int J Climatol 43(8):3782–3798
74. Wang C, Enfield DB (2003) A further study of the tropical Western Hemisphere warm pool. J Clim 16(10):1476–1493
75. Wang C, Lee SK, Enfield DB (2007) Impact of the Atlantic warm pool on the summer climate of the Western Hemisphere. J Clim 20(20):5021–5040
76. Wang P, Yang Y, Tang J, Leung LR, Liao H (2021) Intensified humid heat events under global warming. Geophys Res Lett, *48*(2), e2020GL091462.
77. WMO (2024) Climate change indicators reached record levels in 2023. https://wmo.int/
78. Wong ML, Battisti DS, Liu X, Ding Q, Wang X (2023) A North–South Dipole Response of the South Atlantic Convergence Zone During the Mid-Holocene. *Geophys Res Lett*, *50*(23), e2023GL105130
79. Xia Y, Li Y, Guan D, Tinoco DM, Xia J, Yan Z et al (2018) Assessment of the economic impacts of heat waves: a case study of Nanjing, China. J Clean Prod 171:811–819
80. Xu F, Chan TO, Luo M (2021) Different changes in dry and humid heat waves over China. Int J Climatol 41(2):1369–1382
81. Yarnal B (1993) Synoptic climatology in environmental analysis. CRC
82. Zhang J, Wu L (2011) Land-atmosphere coupling amplifies hot extremes over China. Chin Sci Bull 56(31):3328–3332

Figures

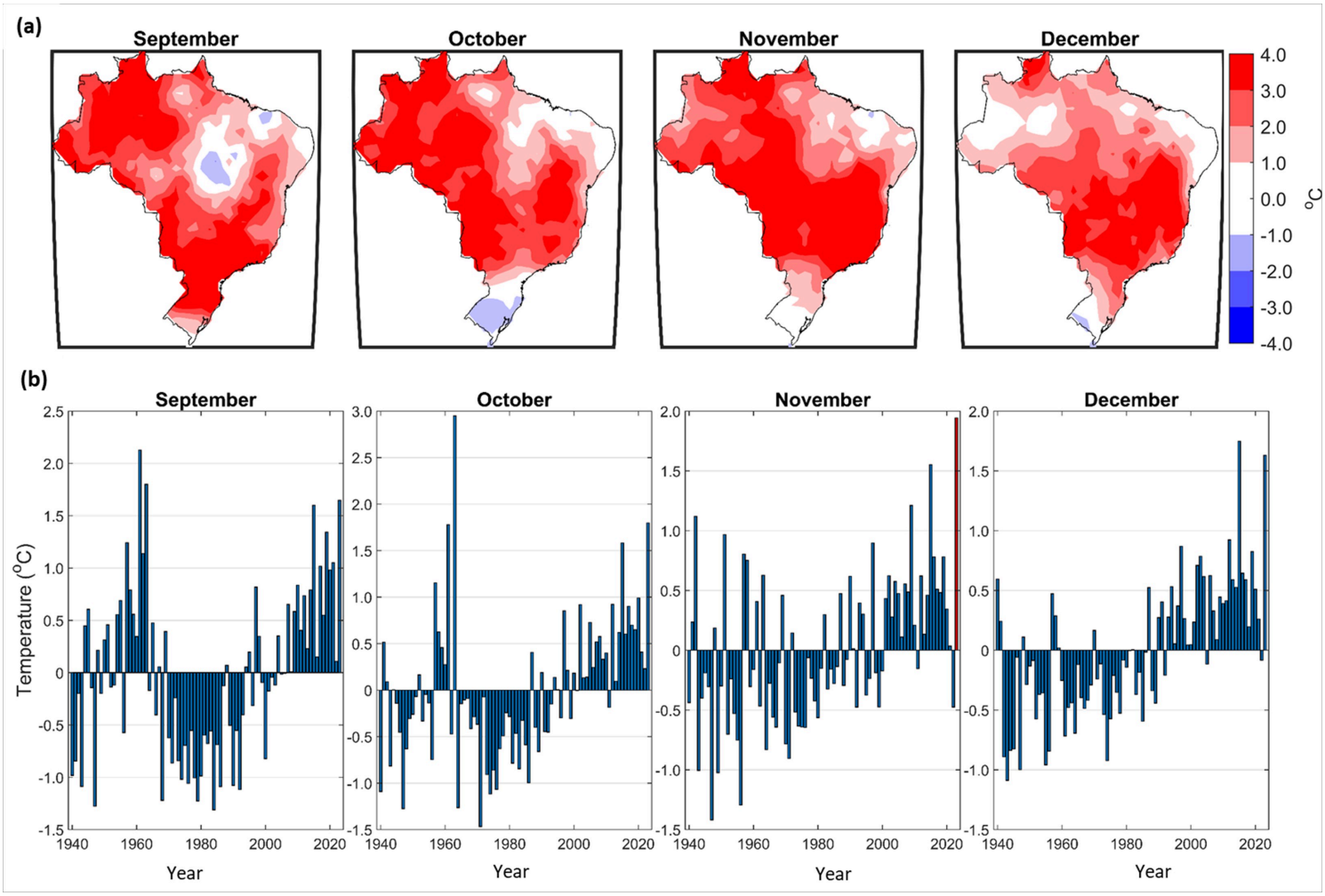


Figure 1

(a) Spatial anomaly of 2-m mean monthly temperature in Brazil during the 2023 Austral spring and early summer months (September to December), and (b) time series of 2-m temperature anomalies averaged over Brazil for the 2023 spring and early summer months (1940 – 2023). Anomaly is calculated relative to the 1940 – 2023 climatology. The anomalous November 2023 temperature is shown by a red bar. Surface temperature data was obtained from ERA5 reanalysis.

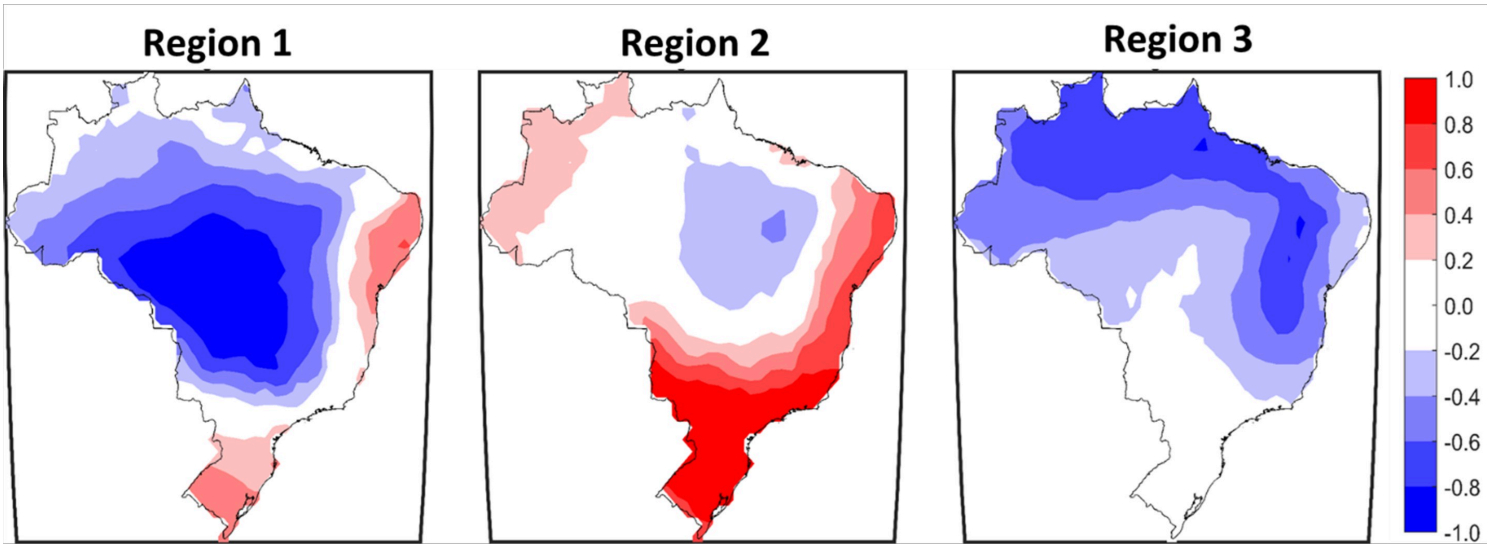


Figure 2

Spring and early Summer temperature coherent regions from ERA5 (1940 – 2023). Color is the PC loadings magnitudes.

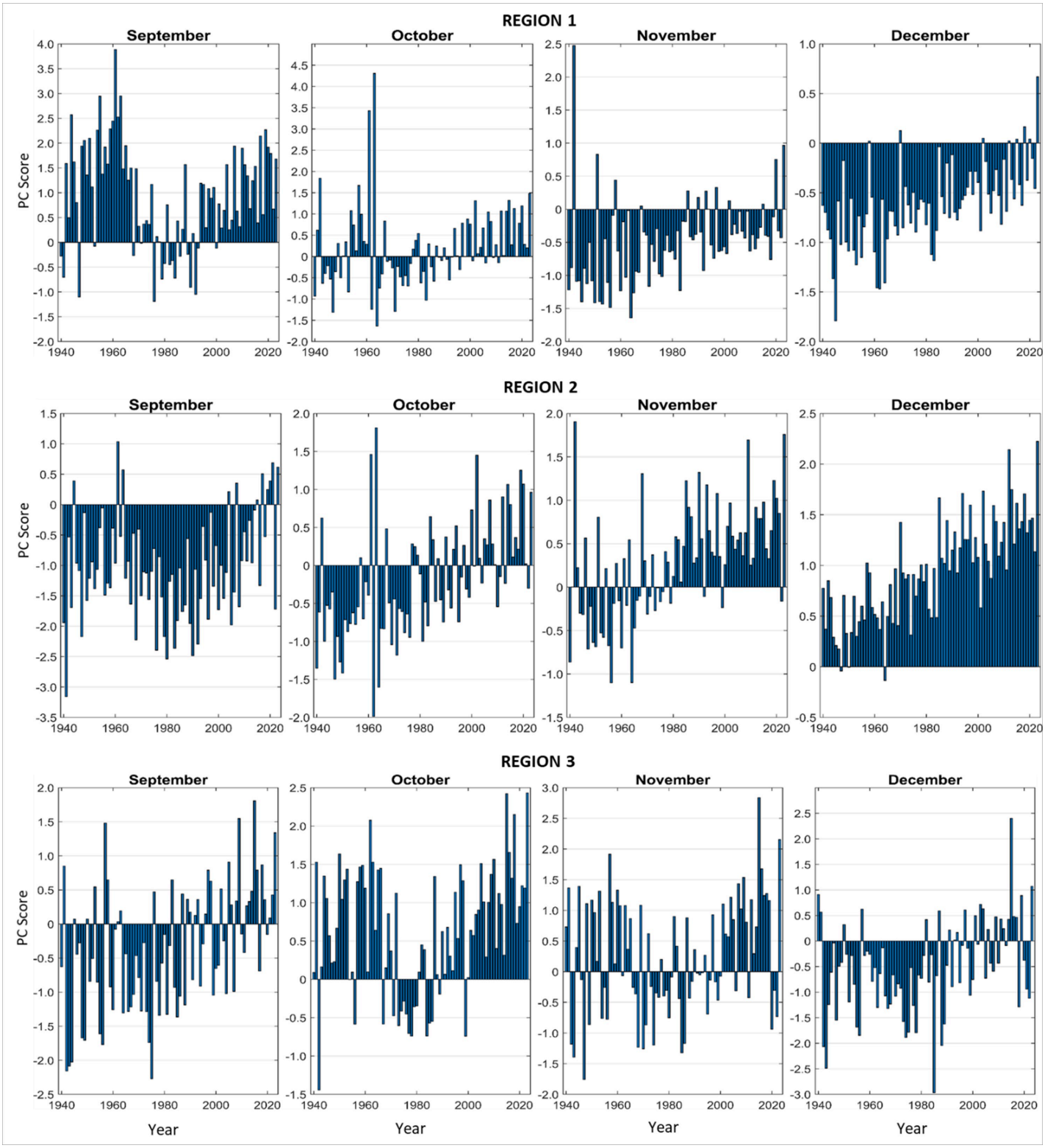


Figure 3

Monthly (spring and early summer) PC Scores for the temperature coherent regions in Figure 2 (1940 - 2023).

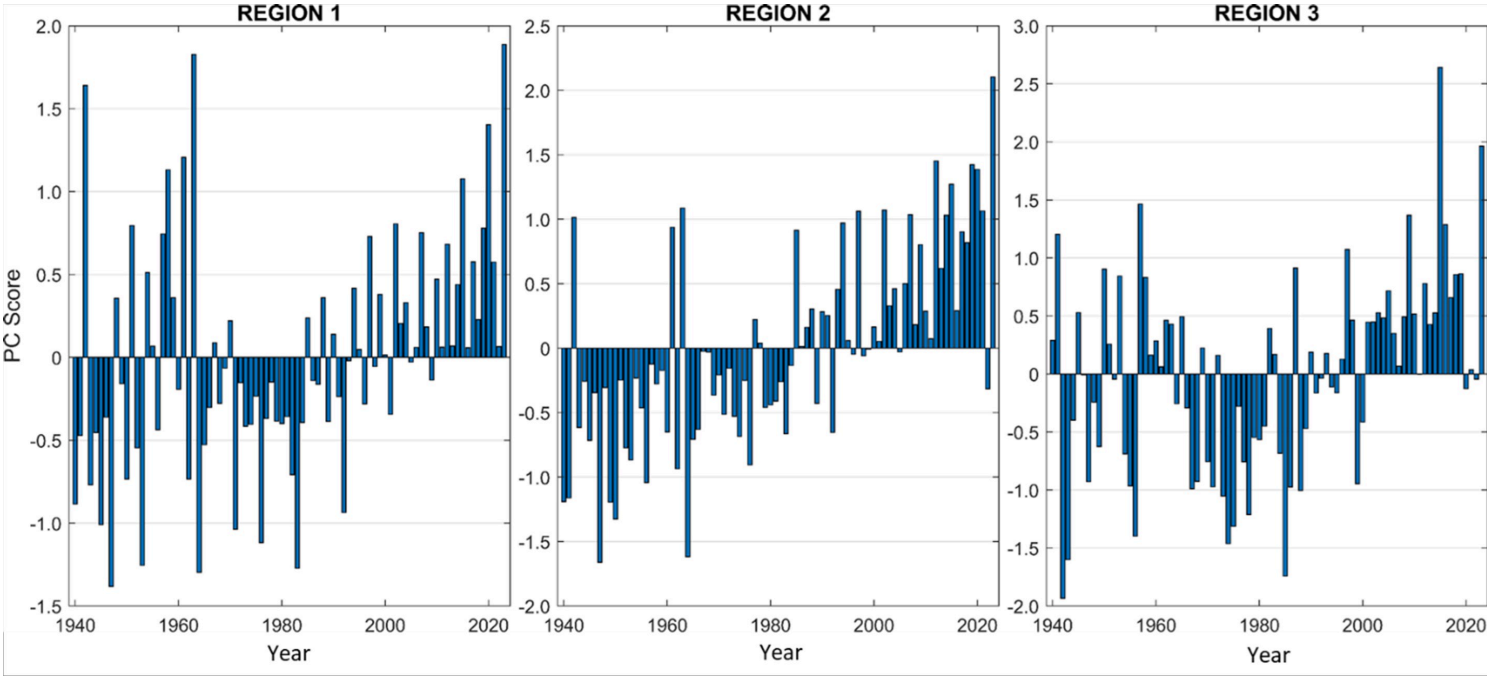


Figure 4

Seasonally averaged standardized PC scores for the temperature coherent regions in Figure 2 (1940 – 2023).

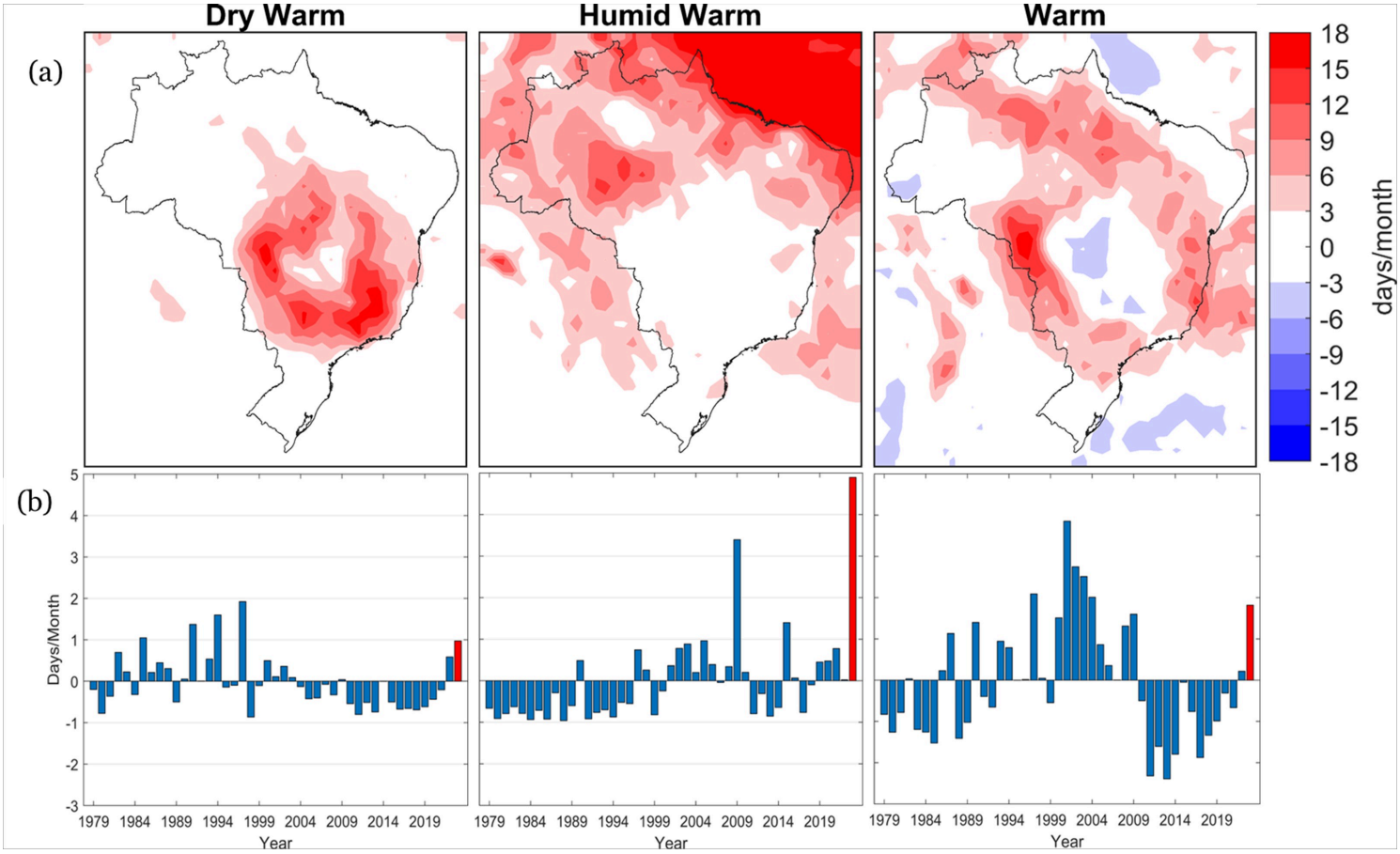


Figure 5

(a) spatial anomaly of AMs during the heat wave, relative to the long-term mean for November (b) The time-series of anomalous November AMs (relative long-term mean November temperature) averaged for Brazil. Anomaly is calculated relative to the 1940 – 2023 climatology. The anomalous November 2023 AMs are shown by a red bar.

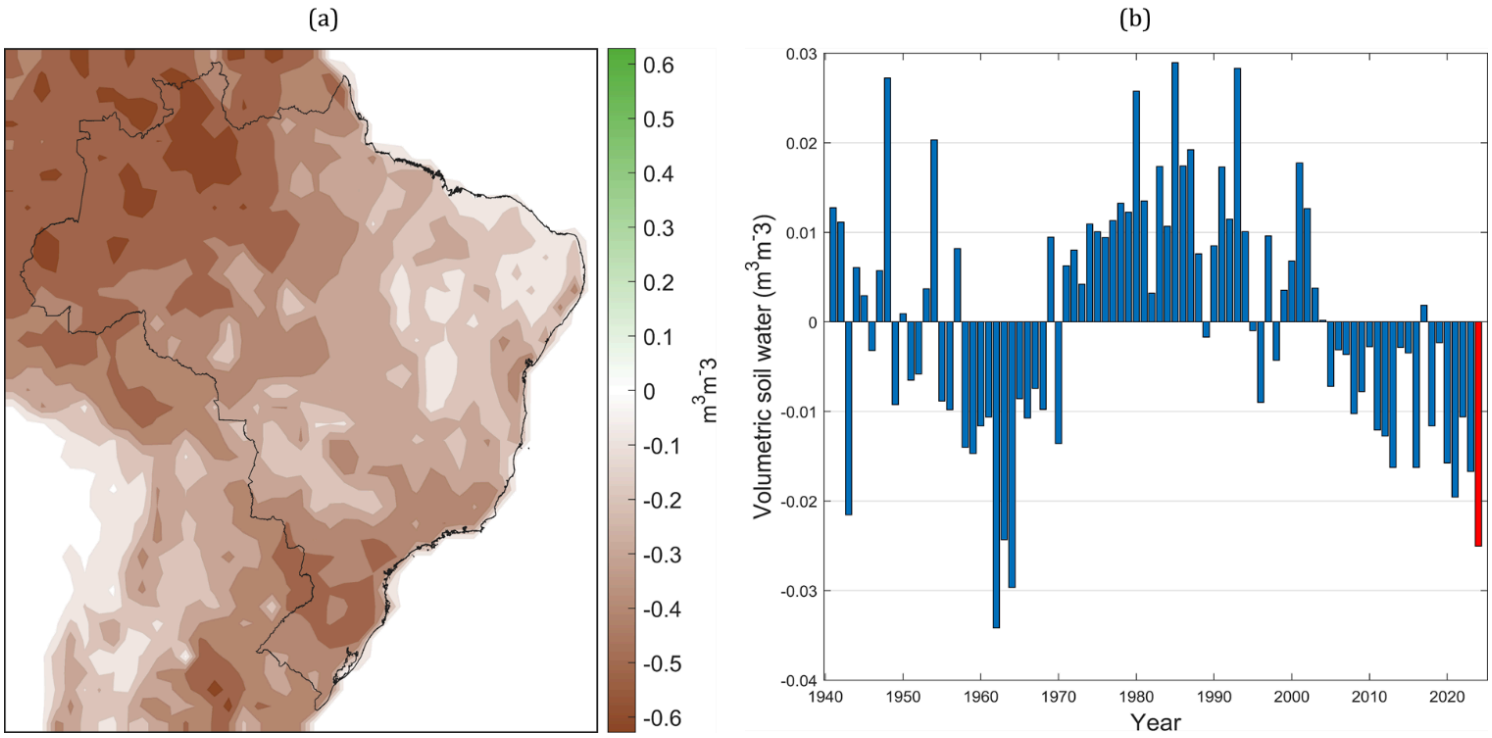


Figure 6

(a) Spatial anomaly of volumetric soil water (top layer) in Brazil during the 2023 November heat wave. (b) Time series of anomalous November volumetric soil water (top layer). Anomalies averaged over Brazil for all November months (1940 – 2023). Anomaly is calculated relative to the 1940 – 2023 climatology.

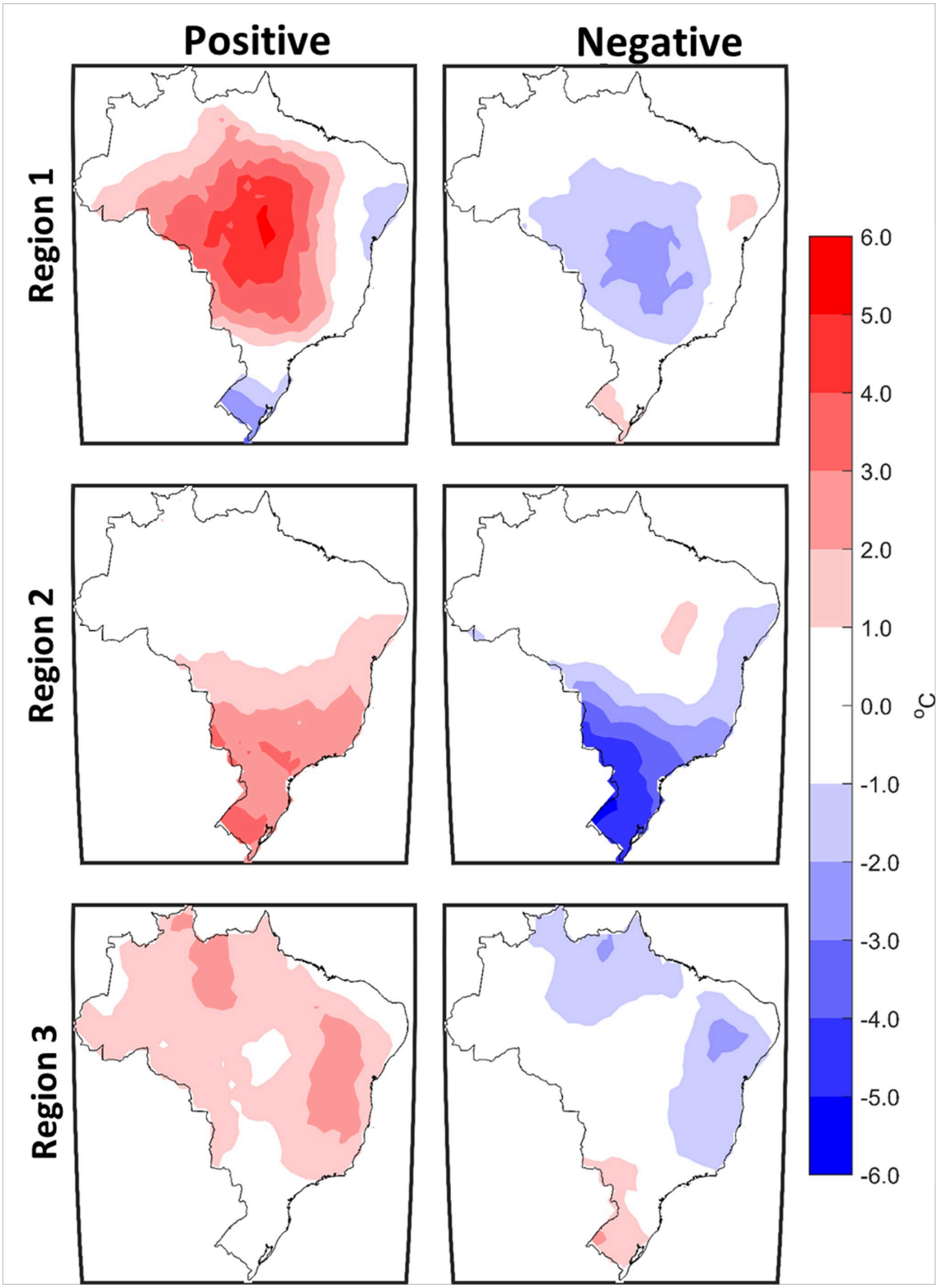


Figure 7

Composite anomaly maps of spring and early summer temperature in each region.

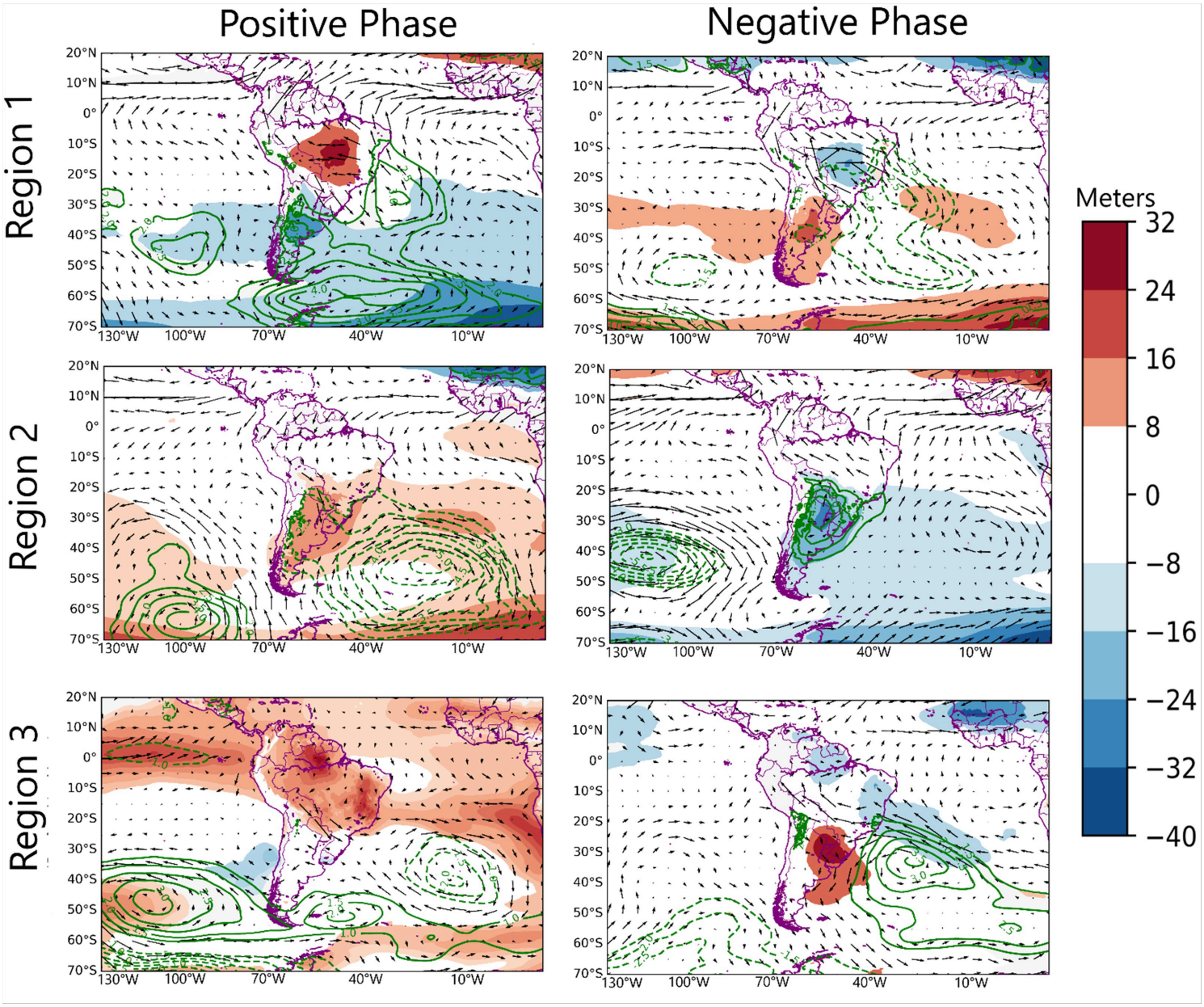


Figure 8

Composite anomaly maps of MSLP (green contours), 850 hPa wind (black vectors), and atmospheric layer thickness between 850 and 1000 hPa (color) for spring and early summer temperature variability patterns in Figure 2. Dashed (thick) contour lines represent below average (above average) MSLP. Contour interval is 0.5 hPa. Only regions with values exceeding the 90% confidence limit, based on the permutation test are shaded.

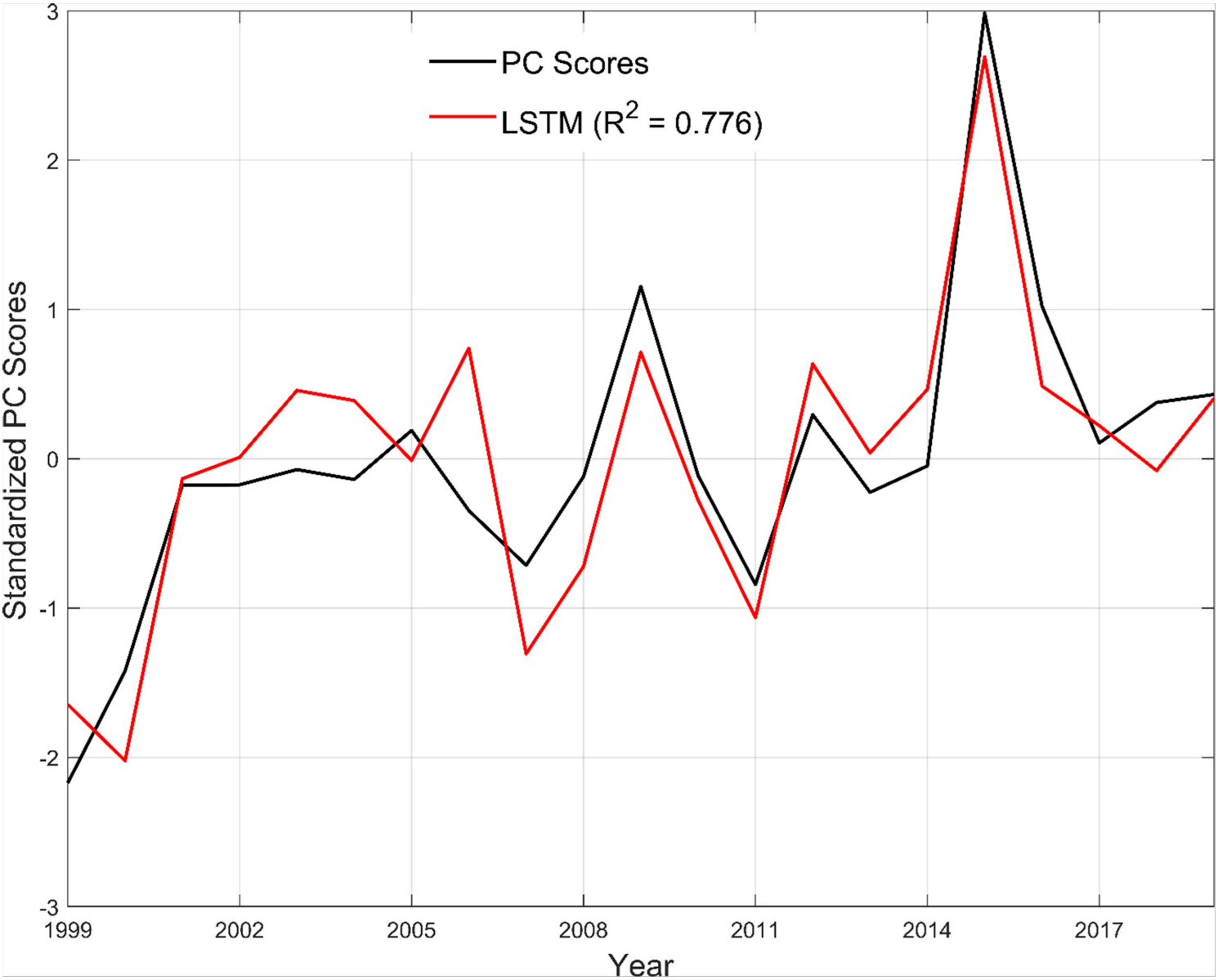


Figure 9

Actual and Predicted PC scores of Region 3 based on the monthly indices of selected climate modes using Long short-term memory (LSTM) neural network model for the last 30% of the data (1999 – 2019).

Supplementary Files

This is a list of supplementary files associated with this preprint. Click to download.

- SupplementaryMaterial.docx